European Polymer Journal 98 (2018) 483–491

Contents lists available at ScienceDirect

European Polymer Journal

journal homepage: www.elsevier.com/locate/europolj

Fabrication of core-shell structured nanofibers of poly (lactic acid) and poly (vinyl alcohol) by coaxial electrospinning for tissue engineering

Hamad F. Alharbi[a,*], Monis Luqman[a], Khalil Abdelrazek Khalil[b], Yasser A. Elnakady[c], Omar H. Abd-Elkader[c], Ahmed M. Rady[c], Nabeel H. Alharthi[a], Mohammad R. Karim[d]

[a] Mechanical Engineering Department, King Saud University, P.O. Box 800, Riyadh 11421, Saudi Arabia
[b] Mechanical Engineering Department, College of Engineering, University of Sharjah, Sharjah 27272, United Arab Emirates
[c] Department of Zoology, College of Science, King Saud University, Riyadh 11451, Saudi Arabia
[d] Center of Excellence for Research in Engineering Materials, Advanced Manufacturing Institute, King Saud University, Riyadh 11421, Saudi Arabia

ARTICLE INFO

Keywords:
Poly lactic acid
Poly vinyl alcohol
Coaxial electrospinning
Core-shell structured fibers
Tissue regeneration

ABSTRACT

Poly Lactic Acid (PLA) nanofiber scaffold has enjoyed great interest as a candidate bioactive material for tissue regeneration. However, the hydrophobic nature of PLA and its weak mechanical properties with poor ductility and low strength hinder its practical applications. In this study, coaxial electrospinning was used to fabricate core-shell composite nanofibers with PLA in the core and PVA in the shell with significant enhancements in the surface wetting and mechanical properties. More specifically, the core/shell-structured PLA/PVA nanofiber mat exhibited excellent hydrophilic properties with a water contact angle of 27 ± 1.5° compared to 110° ± 2.5° for pristine PLA. Moreover, the fabricated composite nanofibers displayed nearly 254% and 175% increase in tensile strength and strain at failure, respectively, compared to pristine PLA (14.5 MPa vs. 4.1 MPa for tensile strength and 110% vs. 40% for ductility). The coaxial electrospun PLA(core)/PVA(shell) nanofibers also showed suitable properties for proliferation, and attachment of human embryonic kidney cells (HEK-293). These excellent combined mechanical, surface wetting, and cytocompatibility properties clearly demonstrate the potential applications of the synthetic core-shell PLA/PVA composite nanofibers in biomedical and tissue regeneration.

1. Introduction

In the last 20 years, synthetic biopolymers have been widely used in various important applications such as electronics, food packaging, bioplastics, coating, and medical usage due to their excellent mechanical, electrical, and biological properties [1,2]. In tissue engineering and regenerative medical applications, an artificial biocompatible and biodegradable fiber has gained attention due to its unique replacing nature when a new tissue is regenerated [3,4]. In particular, nanofiber scaffolds of Poly Lactic Acid (PLA) thermoplastic non-toxic materials have received large interest predominantly as an emerging material for utilization in the fields of regenerative medicine [5–7]. However, the hydrophobic nature and weak mechanical properties of PLA with poor ductility and low strength limit its widespread use in biomedical applications.

The hydrophilicity is particularly important in tissue engineering because adhesion, protein absorption, and cell growth are strongly influenced by the surface wetting properties [8,9]. Several methods have been proposed to modify the surface properties of PLA such as plasma treatment [10–12] and the incorporation of highly hydrophilic materials with PLA [13]. Abdal-hay et al. [3] has shown that the hydrophilicity of PLA can be improved by incorporating hydroxyapatite (HA) with PLA by air jetting spinning. It was reported that the contact angle decreased from about 130° for PLA to about 80° for nanoHA/PLA. Yang et al. [14] has modified the surface wettability of electrospun PLA/cellulose scaffold by applying a coating layer of polydopamine (PDA). The PDA-coated composite nanofibers were reported to be completely hydrophilic resulting in significant enhancements of the adhesion, proliferation, and cell growth. In another study, the deposition of thin poly (vinyl alcohol) (PVA) layer onto post electrospun PLA nanofibers using hydrothermal approach has been shown to dramatically improve the hydrophilicity of PLA [15]. The measured contact angle of the fabricated PVA-coated PLA nanofiber mats was about 36° ± 1.5°. Wang et al. [16] has used poly(γ-benzyl-L-glutamate) (PBLG) to modify PLA by blending and improved its surface wettability. The water contact angle of the electrospun PBLG/PLA fiber membranes was about 79° compared to 91° for PLA.

Besides the absence of hydrophilic characteristic of PLA, this

* Corresponding author.
E-mail address: harbihf@ksu.edu.sa (H.F. Alharbi).

https://doi.org/10.1016/j.eurpolymj.2017.11.052
Received 5 October 2017; Received in revised form 12 November 2017; Accepted 29 November 2017
Available online 02 December 2017

material has poor elongation at break and low ultimate strength which limit its successful implementation in applications with large plastic deformation [5,17–19]. In this context, extensive efforts have been directed toward the synthesis of PLA-based composite biopolymers with improved mechanical properties [20–22]. Coaxial Electrospinning technique is perhaps one of the most cheapest and effective process for producing biopolymer composite fibers with very small diameters [23–26]. A good review of the coaxial electrospinning and their different applications can be found in Refs. [27,28]. In this study, our main objective is to use this process for the incorporation of PVA with PLA materials in a core-shell structure to enhance the mechanical and hydrophilic properties of PLA nanofibers while keeping its good biological properties. The PVA was selected because it has excellent surface wetting and mechanical properties [29]. Thus, by combining PLA and PVA polymers in a core–shell structure, the composite fibers are expected to have the structural and hydrophilic benefits of PVA and the biological properties of PLA. To conduct a thorough study, four different electrospun nanofibers were fabricated via electrospinning including (1) core-shell structure with PVA in the core and PLA in the shell, (2) core-shell structure with PLA in the core and PVA in the shell, (3) pristine PLA, and (4) pristine PVA. The surface wetting, mechanical, and biological performance for each class of these nanofibers were characterized using contact angle measurements, tension tests, and cells growth/attachment activities, respectively.

2. Experimental procedures

2.1. Fabrication of core-shell structure of PVA and PLA composite nanofibers

2.1.1. Materials

The materials used for the synthesis work in this study were PLA granules supplied by Green Chemical Co. (Seoul, Korea), Triton X-100 obtained from Loba Chemie Pvt. Ltd. (India), 99.9% hydrolysed PVA pellets, Trichloromethane 99.8%, and ethanol monomers purchased from Sigma-Aldrich (USA).

2.1.2. Coaxial electrospinning

In this study, we fabricated four different electrospun nanofibers including (1) core-shell structure of PVA/PLA, (2) core-shell structure of PLA/PVA, (3) pristine PLA, and (4) pristine PVA. The PVA solutions were prepared by dissolving Poly Vinyl Alcohol morsels in distilled water and ethanol with a ratio of 9:1. The mixture was heated at 75 °C for about 1 h. The viscous solution of 10 wt.% was obtained and cooled to room temperature. In order to reduce the OH bonding, few droplets (~3) of Triton X-100 were spurted into the PVA solution and stirred for 15 mins. Furthermore, another viscous solution of 8 wt.% Poly Lactic Acid was prepared by adding chloroform and Dimethylformamide (DMF) with a ratio of 8:2. Stirring it at room temperature for about 5 h. DMF was added to PLA solution in order to increase the conductivity and dielectric constant [19].

A coaxial apparatus containing two concentric needles was used to fabricate the core/shell structure of PVA/PLA and PLA/PVA nanofibers. The diameters of the inner and outer needles were 0.8 mm and 1.2 mm, respectively. The inner needle was 0.25 mm longer than the outer needle. The PVA and PLA solutions were collected in separate two 20 ml syringe pumps and delivered at feeding rates of 0.1 ml/h and 0.2 ml/h for the core and shell, respectively. An aluminum cylindrical rotating drum was used to collect the coaxial electrospun nanofibers with a distance of 14 ± 1 cm between the needle tip and the collector. During the coaxial electrospinning, the applied voltage was 19 kV and the rotating speed of the collecting drum was 80 rpm. The electrospinning process runs for at least 7 h, which resulted in the formation of thick non-woven nanofiber membrane.

The pristine PLA and PVA nanofibers were fabricated using the same PVA and PLA solutions described above via single-nozzle electrospinning method. The process parameters for producing both pristine PLA and PVA electrospun nanofibers were set to 0.2 ml/h feeding rate, 20 kV applied voltage, and 14 cm spinneret-to-collector distance. Both PVA and PLA nanofiber membranes were taken out from electrospinning device and heated in a furnace at 50 °C.

2.2. Measurement and characterization

2.2.1. Morphological observation

The nanofiber morphology was observed using JSM-7600 Field-Emission Scanning Electron Microscope (FE-SEM) supplied by JOEL Ltd., Japan. The samples were first Platinum coated using sputter coater and observed at an acceleration voltage range of 5–15 kV. Transmission Electron Microscopy (TEM) analysis was conducted on nanofiber samples to reveal the coaxial nature using TEM JSM-2100F. The TEM samples were prepared by collecting nanofibers directly onto the copper grids.

2.2.2. Thermal analysis

Differential Scanning Calorimetry (DSC) analysis was performed on all four types of electrospun samples produced in this study (pristine and core/shell structures) under nitrogen atmosphere. Samples weighing 6–8 g were placed in alumina pans and heated from 24 °C to 600 °C at a heating rate of 10 °C/min in SDT Q600 machine supplied by TA Instruments, USA. Glass transition temperatures (Tg) were measured. Furthermore, Thermogravimetric analysis (TGA) was conducted on electrospun samples using SDT Q600 machine supplied by TA Instruments, USA. The samples were heated from room temperature to 600 °C at a heating rate of 10 °C/min under nitrogen atmosphere.

2.2.3. Fourier-transform infrared spectroscopy

Fourier transformed infrared spectroscopy (FTIR) was conducted on pristine as well as coaxial nanofiber mats to identify phase structures and molecular properties using VERTEX70 machine supplied by BRUKER, USA.

2.2.4. Surface wettability measurements

Static water contact angle test was conducted at room temperature on nanofiber samples to regulate surface hydrophilicity of nanofiber mats using Optical tensiometer, supplied by Dyne Technology, U.K. A drop of 3 µl distilled water from stainless steel needle was plummeted on a 40 × 40 mm^2 cut surface of pristine and coaxial electrospun mats. The angular deflections were video recorded every 30 s to determine the contact angles of nanofiber mats. The average of five readings taken at different areas for each sample was taken as the contact angle.

2.2.5. Mechanical testing

The mechanical properties of the pristine PLA, PVA and core/shell-structures of PVA/PLA and PLA/PVA nanofiber mats were determined using a uniaxial tensile test. Samples of each type were cut in dog bone shape according to ASTM D638-10 type-5 with an initial length of 40 mm and thickness of 1 mm. The tests were performed on a micro-tensile test machine (MTD-500 PLUS) at room temperatures at a crosshead speed of 10 mm/min. The test runs until sample failure while recording the force and elongation. To confirm reproducibility of the data, five sample measurements of each nanofiber mats were considered.

2.2.6. Cell study related methods

2.2.6.1. General culture conditions. For the cytotoxicity assay, we used human embryonic kidney cells (HEK-293). Cells were growing in Dulbecco's Modified Eagle's (DMEM) medium containing 10% fetal bovine serum, 2 mM L-glutamine, and 1% Penicillin/Streptomycin. The cultivation temperature was 37 °C, at approximately 99% humidity atmosphere.

2.2.6.2. Toxicity assay. We performed proliferation assay according to the methods of Mosmann [30]. Briefly, cells (5×10^4 cells/ml) were cultivated in the absence and the presence of the polymer discs (12 mm in diameter) in 24-well plates for four days. The MTT was added to the cells, and the cells were incubated under growth conditions for additional two hours. The medium was then removed and the cells were washed two times in Phosphate buffered saline (PBS). The formed formazan crystals were dissolved in Isopropanol/HCl. The absorbance was measured at 570 nm using a plate reader. The intensity of the culture is proportional to the metabolic activity of the cells and the cell number.

2.2.6.3. SEM protocol. Cells were fixed in buffered aldehyde containing 2.5% Glutaraldehyde, and 0.2 M Sodium Cacodylate (pH 7.2). The fixed cells were rinsed three times each for five minutes in a Sodium Cacodylate buffer solution (0.04 g/ml Sodium Cacodylate in 0.2 N HCl). Post- fixation was performed in one percentage Osmium tetra oxide aqueous solution, containing 0.1 M Sodium Cacodylate buffer solution. Dehydration of the samples were done using graded Ethanol series (25, 50, 75, and 100%). Finally, the samples were dried using Critical Point Dryer (CPD), mounted on specimen stabs, and coated with Gold (Thickness 3 nm). Sample examination was done using a high-performance, scanning electron microscope (JSM-6380 LA- Japan) and analyzed using Smile ShotTM software (JEOL- Japan).

3. Results and discussion

3.1. Morphological aspects

The morphologies of the pristine PLA, PVA and core/shell-structures of PVA/PLA and PLA/PVA nanofiber mats were examined using FE-SEM as shown in Fig. 1. The diameters of the pristine and coaxial electrospun nanofibers were estimated to be 138 ± 10 nm and 165 ± 10 nm, respectively. It was noted that the diameter of the fibers increased slightly during the co-axial electrospinning. For the core-shell structure with PVA in the core and PLA in the shell, it was observed that few areas have broken shell due to the brittle nature of PLA. The core structure of PVA was clearly revealed in these locations with broken PLA shell. The break of PLA fibers into short porous structures when immersed in aqueous solutions were reported in previous studies and related to the hydrolysis of aliphatic polyesters [31,32]. The core/shell structure of the nanofibers produced via coaxial electrospinning technique was revealed using TEM analysis as shown in Fig. 2. In order to differentiate between the core and shell fibers in the TEM analysis only, silver nanoparticles were added to the shell polymer solution before electrospinning. The analysis articulates that the core PLA or PVA was restricted at center with a diameter of 35 ± 5 nm and shell fiber as an external layer with a diameter of 165 ± 10 nm. Moreover, it was observed that the pristine PLA and PLA shell fibers have a porous structure as shown in Fig. 3.

3.2. Thermal analysis

Thermal analysis of pristine PVA, PLA and core/shell-structured PLA/PVA and PVA/PLA nanofiber mats were investigated by thermogravimetric (TGA), differential thermogravimetric (DTG) and differential scanning calorimetry analysis. Fig. 4(A and B) demonstrates the TGA and DTG curves obtained in a range of 20–600 °C with a heating rate of 10 °C/min. The PVA polymer nanofibers showed three stages of degradation. In the first stage, moisture loss was observed from 25° to 280 °C. The second (side chain decomposition) and third (main chain decomposition) stages were observed at 290–360 °C and 420–450 °C, respectively. Furthermore, the pristine PLA nanofiber showed a single-stage degradation at 368 °C. On the other hand, the core/shell structures of both PLA/PVA and PVA/PLA nanofibers showed nearly two steps of degradation as shown in Fig. 4(A and B). These degradations occurred at about 298–301 °C and 430 °C, respectively. It is clear that the two core/shell- structured nanofiber mats exhibited almost similar trends in their thermal properties. It is interesting to note that the shape of the TGA/DTG curves for the coaxial composite nanofibers of PLA/PVA and PVA/PLA combines the main characteristics of both pristine PLA and PVA with an initial steep decrease in slope (similar to PLA) followed by gradual degradation (similar to PVA). These TGA results provide further evidence to the successful fabrication of core/shell composite nanofibers of PVA and PLA via coaxial electrospinning technique. It can conclude from the thermal properties that the PLA/PVA composite nanofibers mats possese lower decomposition temperatures than that of prisine mats.

Fig. 5 illustrates the results of the DSC measurements. The pristine PLA curve indicates that the glass transition temperature and melting point occur at 66.6 °C and 154 °C, respectively. The pristine PVA curve shows that the glass transition temperature overlapped with water loss peak and can be measured at about 58 °C and the melting point at 210 °C. However, the results of the core/shell structures of both PLA/PVA and PVA/PLA nanofibers were similar in a melting temperature with multiple changes in the heat flow curves. The glass transition temperature of the coaxial composite nanofibers of PLA/PVA and PVA/PLA observed at 58 and 53 °C, while, the melting point was about 145.6 °C, respictively. Once again, the DSC measurements of the core/shell structures of PVA and PLA reported in this study support the successful application of coaxial electrospinning for fabricating such composite nanofibers. Hence, the composite nanofibers mats combined from PLA and PVA have lower melting temperature and glass transition temperature than pristine PLA nanofibers mat. Due to the viscoelastic or viscoplastic nature of polymers, the mechanical properties of polymer networks are in relation to the melting temperature and glass transition temperature (Tg) of the polymers. Hence, it is expected that such this behaviour may have an effect on the mechanical preoperties of the prepared materials.

3.3. FTIR spectra of nanofiber mats

FTIR spectra were obtained for pristine PLA, pristine PVA, core/shell-structured PVA/PLA, and core/shell-structured PLA/PVA nanofibers as shown in Fig. 6. The spectra of the pristine PVA possessed bands at around 3367 cm^{-1} (OH stretching), 2935/2905 cm^{-1} (CH_2 asymmetric/symmetric stretching), 1427 cm^{-1} (CH_2 bending), 1089 cm^{-1} (C—O stretching), and 833 cm^{-1} (CH bending) [15,33,34]. Furthermore, the bands of pristine PLA occur at around 2943/2995 cm^{-1} (CH_3 asymmetric/symmetric stretching), 1749 cm^{-1} (C═O stretching), 1452 cm^{-1} (δCH_3), 1183 and 1080 cm^{-1} (C—O—C stretching), 1043 cm^{-1} (C—CH_3 stretching), 865 cm^{-1} (C—COO stretching), and 755 cm^{-1} (δC═O in-plane bending) [19,35,36]. However, the spectra of the PVA/PLA and PLA/PVA core-shell nanofibers showed different intensities for most of the peaks of both PLA and PVA, indicating the presence of both materials in the composite nanofibers.

The strong intensity of the hydroxyl group (characteristic for PVA ~3367 cm^{-1}) band was not clearly seen in the spectra of the core-shell PVA/PLA composite mat indicating the absence of PVA on the surface of the fibers. Similarly, the intensity of the carboxyl group (characteristic for PLA ~1749 cm^{-1}) band was hardly seen in the core/shell-structured PLA/PVA. Similar FTIR observations were reported in a previous study for similar material structures [37]. These results may give further evidence for the coaxial nature of the fabricated composite nanofiber mats.

3.4. Contact angle measurement

Poly Lactic Acid (PLA) is biodegradable polymer but its practical applications in artificial tissues and organs are limited due to its hydrophobicity that results in poor cell attachment. The surface wetting properties of nanofiber mats, usually evaluated by contact angle

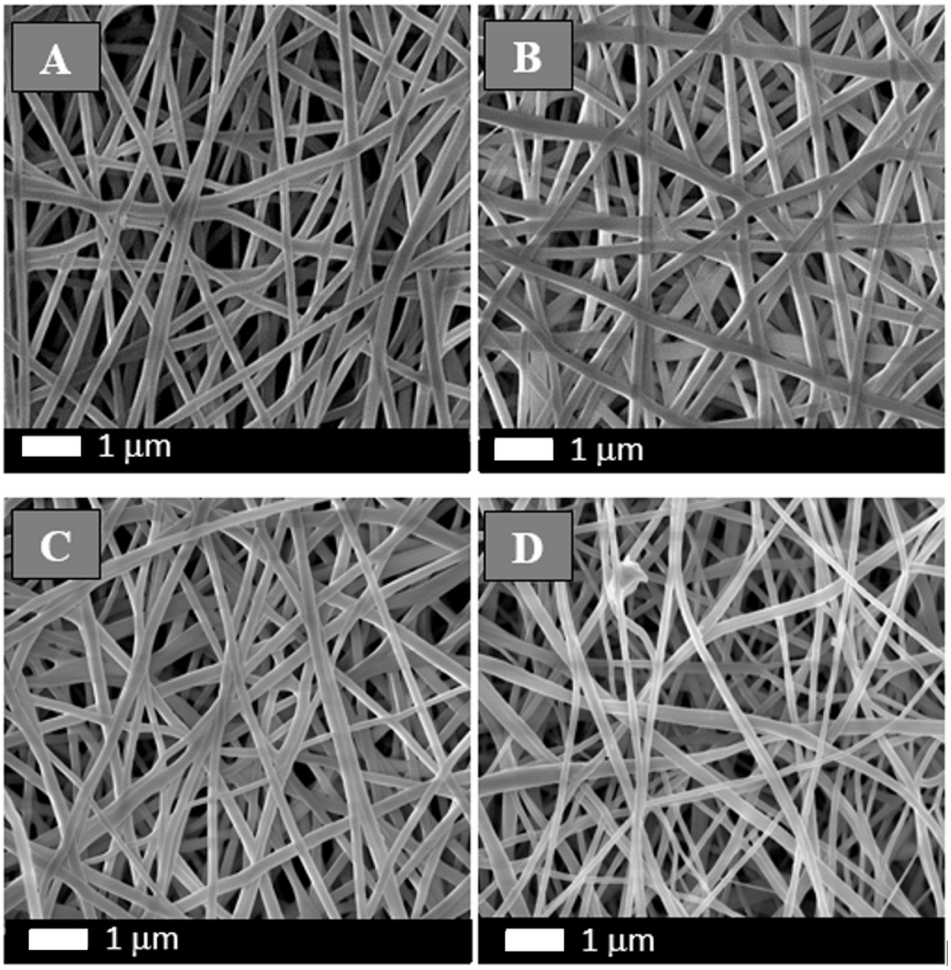

Fig. 1. SEM results of (A) pristine PLA, (B) pristine PVA, (C) core/shell-structured PLA/PVA, and (D) core/shell-structured PVA/PLA.

measurement, have a major impact on their biocompatibility, protein absorption and cell attachment [8–10]. To evaluate the hydrophilicity of the PLA/PVA-based polymer nanocomposites produced in this study, we measure the water contact angle of pristine PLA, PVA and core/shell structures of PVA/PLA and PLA/PVA nanofibers. Fig. 7 reveals the results of these measurements. The pristine PVA polymer is shown to be very hydrophilic with a contact angle of 5° ± 1.5° as shown in Fig. 7(b). In contrast, the inset of Fig. 7(a) shows that the pristine PLA nanofiber mat is hydrophobic with a contact angle of 110° ± 2.5°. Similar results for PLA were reported in other studies [3,15]. The low hydrophilicity of PLA is related to its methyl group [13]. The core/shell-structured of both PLA/PVA and PVA/PLA nanofiber mats were found to have significant improvement in the hydrophilic properties compared to PLA alone. The result showed that when PLA was taken as the core, the outer hydrophilic PVA shell absorbed the water droplet and the angle steeply dragged down to 27° ± 1.5°. For the other core/shell-structured PVA/PLA nanofiber, the porous PLA shell provided channels for the water droplet to pass through and get absorbed by the hydrophilic PVA core fibers resulting in a contact angle of 19° ± 1.5°. The porosity of PLA was observed using the microscopic scanning technique as presented earlier in Fig. 3. It should be noted that the current result of the low contact angle reading for the core/shell-structured PVA/PLA nanofiber mat is not expected if PLA was not porous. For example, the contact angle results of coaxially electrospun polymer nanofibers with hydrophilic gelatin in the core and hydrophobic poly(ε-caprolactone) (PCL) in the shell was comparable to pure

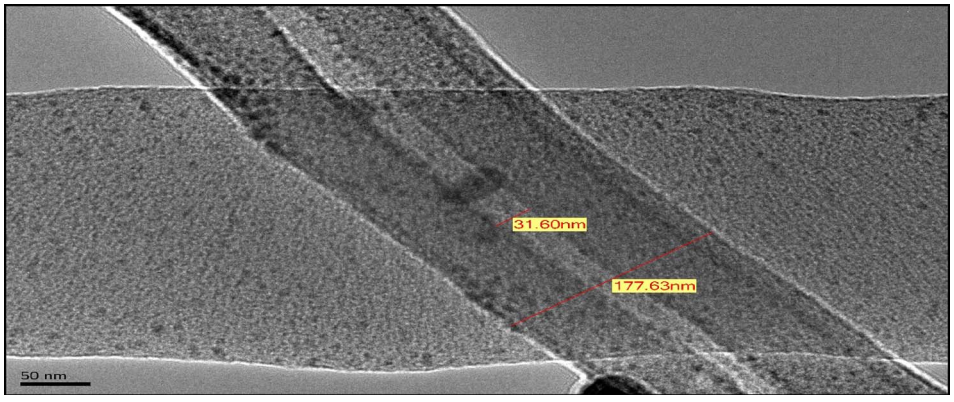

Fig. 2. TEM analysis showing the core-shell structures of the coaxial PVA/PLA nanofibers.

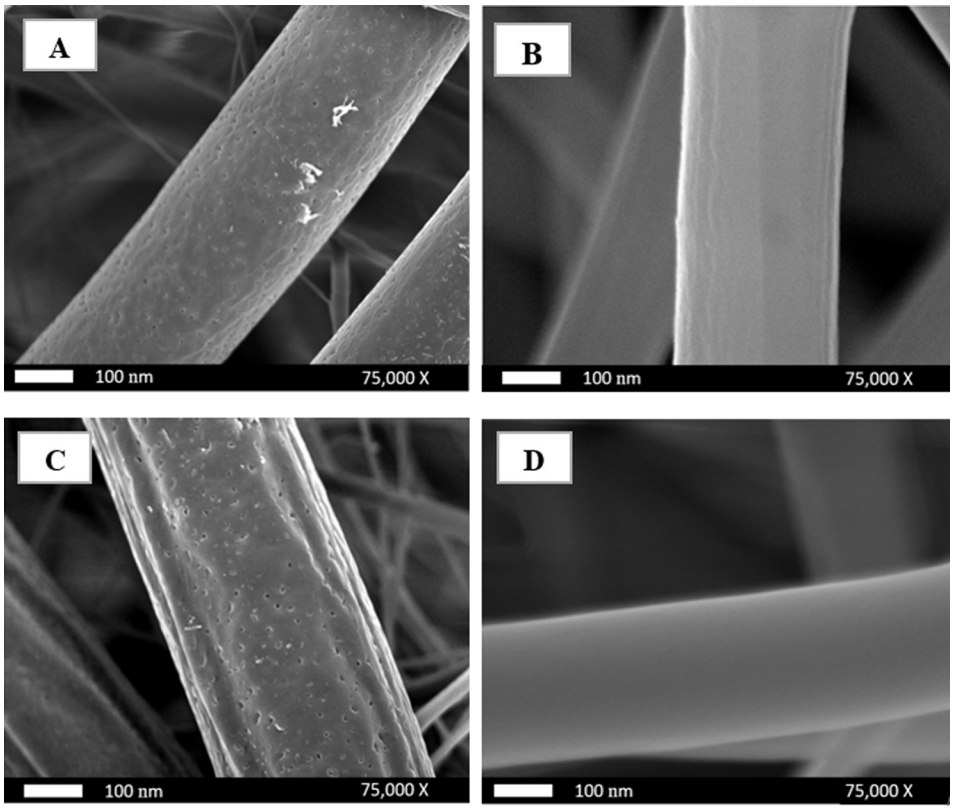

Fig. 3. SEM analysis showing the porous structure of pristine PLA (A) and core/shell-structured PVA/PLA (C). The pristine PVA (B) and core/shell-structured PLA/PVA (D) do not reveal any porosity.

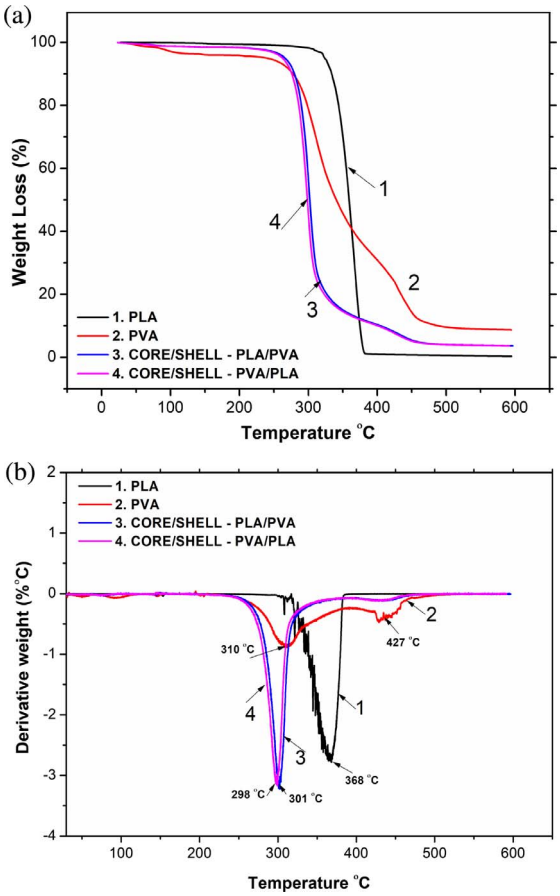

Fig. 4. (A) Thermogravimetric (TGA) and (B) differential thermogravimetric (DTG) curves of pristine (PVA and PLA) and core/shell-structured (PLA/PVA and PVA/PLA) nanofiber sheets.

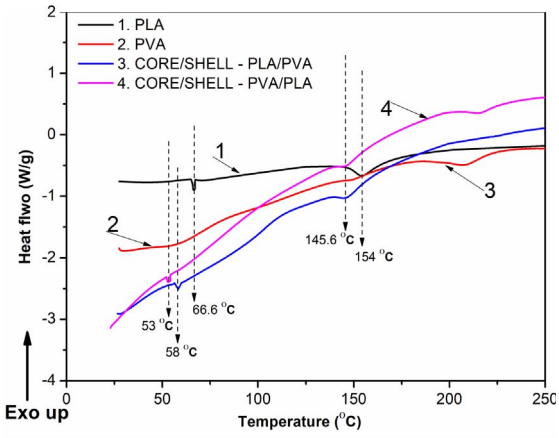

Fig. 5. DSC curves of pristine (PVA and PLA) and core/shell-structured (PLA/PVA and PVA/PLA) nanofiber sheets.

PCL nanofibrous membrane [38]. The remarkable enhancement in hydrophilicity of the PLA-PVA nanocomposite nanofibers fabricated via coaxial electrospinning technology are highly attractive for tissue regeneration technologies.

3.5. Mechanical properties

The mechanical response of the different fabricated electrospun nanofiber mats (pristine PVA, pristine PLA, core/shell-structured PLA/PVA, and core/shell-structured PVA/PLA) were determined by testing the materials in tension until failure. For each group, four repeated tests were performed. Fig. 8 shows the typical stress-strain curves for the single and coaxial electrospun nanofiber sheets made from PVA and PLA polymers. The values of the measured ultimate tensile strength and strain at failure were evaluated form the curves and listed in Table 1. The results clearly reflect the expected weak mechanical properties of

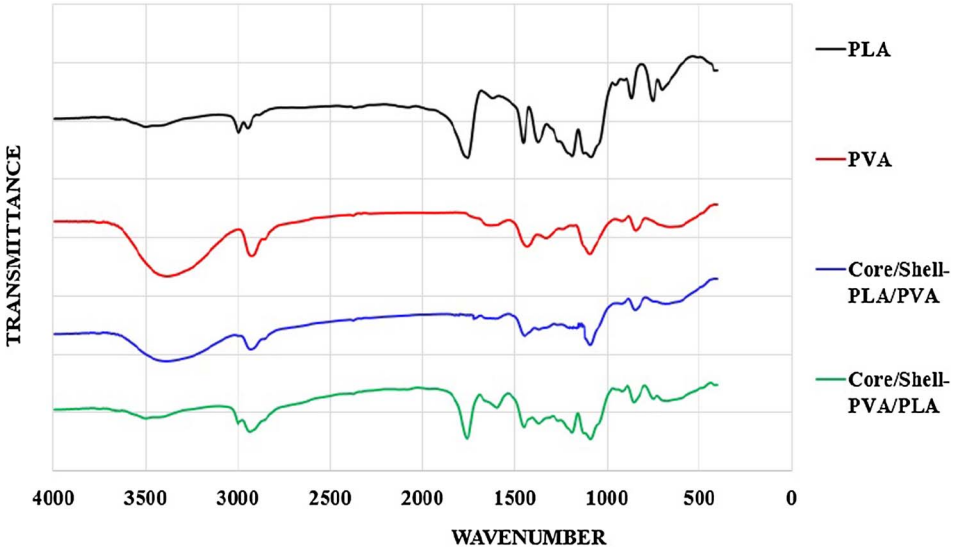

Fig. 6. FTIR spectra of pristine PVA, pristine PLA, core/shell-structured PLA/PVA, and core/shell-structured PVA/PLA.

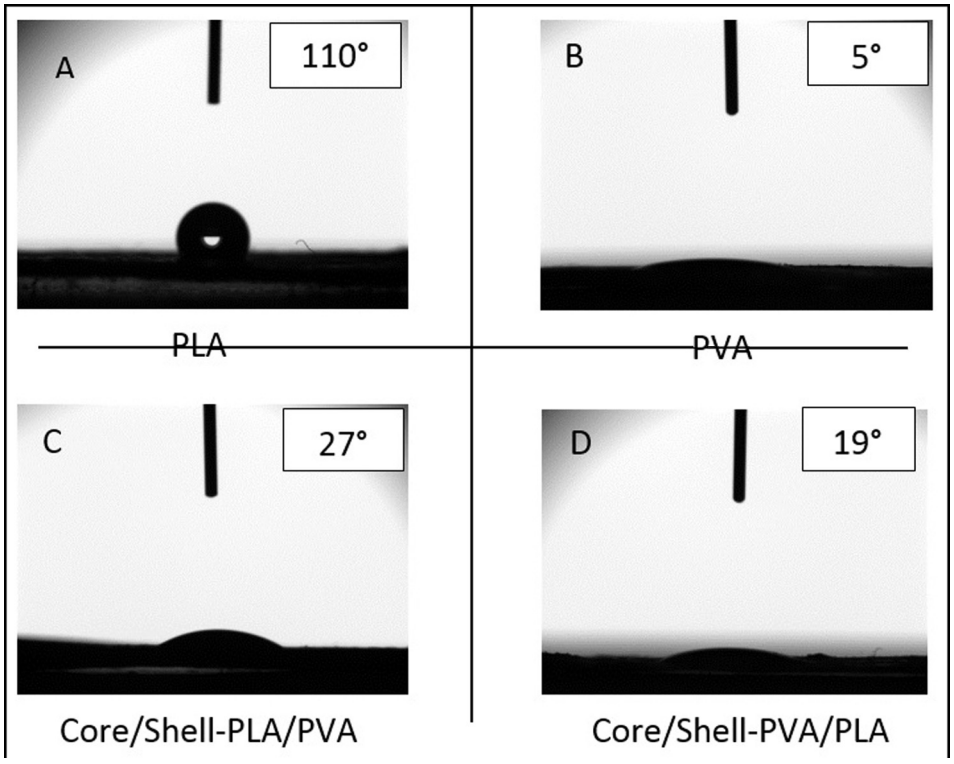

Fig. 7. Contact angle measurements of pristine (PVA and PLA) and core/shell-structured (PVA/PLA and PLA/PVA) nanofiber mats.

the electrospun pristine PLA nanofiber mat compared with PVA. The PLA nanofiber tested in tension has a low ultimate strength of about 4.1 ± 0.15 MPa and poor ductility with a strain at failure of about 40%. On the contrary, the PVA nanofiber has a relative good tensile strength of about 10.1 ± 1.35 MPa and fail at a moderate strain of about 78%. Similar mechanical properties for PVA and PLA were reported in other studies [39–41].

The overall mechanical properties of the core/shell-structured nanofiber mats are expected to depend on the contribution of both the core and shell nanofibers. In this study, it was found that the mechanical response of the composite nanofibers is strongly affected by the type of material in the core and shell. In general, the coaxial electrospun core/shell composite nanofiber sheets produced in this study have attractive mechanical response compared to pristine PVA and PLA. For example, the core/shell-structured PVA/PLA nanofiber mat has a good ultimate strength of about 8.0 ± 1.65 MPa, a value in between those of pristine PLA (4.1 MPa) and pristine PVA (10.1 MPa). However, there was no observed improvement in its ductility compared to pure electrospun PLA. The elongation at failure for this coaxial PVA/PLA core-shell composite nanofiber was about 42%, which is very close to the value of pristine PLA (40%). However, the core/shell-structured PLA/PVA nanofiber mat has superior strength and ductility compared to pristine PLA and PVA. This composite nanofiber mat exhibits a high tensile strength of about 14.5 ± 1.95 MPa and a good ductility with a strain at failure of about 110%. Compared to pristine PLA and PVA nanofiber sheets, it thus displayed, respectively, nearly 254% and 44% increase in tensile strength (14.5 MPa vs. 4.1 MPa and 10.1 MPa), and 175% and 41% increase in strain at failure (110% vs. 40% and 78%). It should be noted that the increase in elongation at break is usually accompanied by a decrease in strength. However, the coaxial electrospun

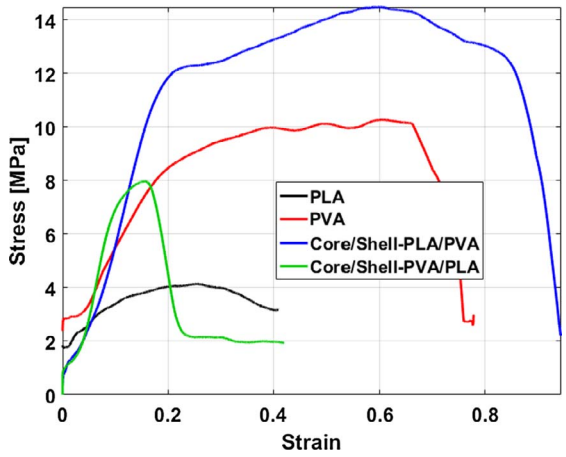

Fig. 8. Typical tensile stress-strain curves of pristine (PVA and PLA) and core/shell-structured (PVA/PLA and PLA/PVA) nanofiber sheets.

Table 1
Values of the measured tensile strength and strain at failure for pristine (PVA and PLA) and core/shell-structured (PVA/PLA and PLA/PVA) nanofiber sheets.

Materials	Tensile strength [MPa]	Strain at failure
Pristine PLA	4.1	0.4
Pristine PVA	10.1	0.78
Core/Shell-PLA/PVA	14.5	1.1
Core/Shell-PVA/PLA	8.0	0.42

core-shell nanofiber mats with PLA in the core and PVA in the shell exhibited significant improvements in both tensile strength and ductility compared to the electrospun PLA or PVA alone.

The mechanical properties of composite core/shell nanofiber sheets are strongly affected by different factors including the type of polymers in the core and shell, chemical and/or physical interactions between the two layers, nanofibers diameter, length, distribution, entanglement, and defects. The experimental quantification of these features in a statistical representative framework and linking them to the mechanical response are challenging. It is thus noted that many of the coaxial composite polymers reported in previous studies exhibit large variability in their mechanical response. For example, Sun et al. [41] has investigated the mechanical properties of core/shell structure of poly (vinyl pyrrolidone) (PVP) and PLA ultrafine fibers produced by coaxial electrospinning and found that the tensile modulus and tensile strength of the core/shell-structured PVP/PLA membrane were lower than those of the electrospun pure PLA membrane. The drop in these properties was attributed to the weak physical interactions among the chains of mixed polymers and the morphology of imperfection. However, Merkle et al. [33,39] has reported an increase in the values of young's modulus and ultimate strength in the core/shell structure of PVA/gelatin composite scaffolds produced by coaxial electrospinning when compared with the PVA or gelatin scaffolds. Such improvements were related to the possible enhancement of the molecular alignment of core PVA by the gelatin shell. In our study, there should be some interactions between the PVA and PLA layers that contribute to the resulting mechanical properties. One possible reason for the improved ductility of the coaxial core-shell composite mats can be related to their lower glass transition temperature compared to both pristine PLA and PVA as shown in Fig. 4. It is known that when decreasing the polymer thermal stability, the polymer becomes soft and ductile. Furthermore, since the mechanical property of the nanofibrous mats can also depend on how they were prepared (e.g. densely packed mat is expected to be stronger), the weight of all electrospun nanofibrous mats with the same dimensions (~10 mm × 10 mm × 0.2 mm) were measured. The weight of the pristine PLA and PVA mats were found to be close to each other (~3.4 mg) while the weight of the coaxial core-shell PLA/PVA and PVA/PLA mats were higher by about 16% and 8%, respectively. This may contribute to the increase in the values of the ultimate tensile strength for the core/shell mat structures of PLA/PVA and PVA/PLA. However, we should mention that the exact underlying mechanisms responsible for the significant improvement in the mechanical properties of the coaxial core/shell-structured PLA/PVA nanofiber mat compared to pure PLA and PVA nanofibers cannot be deduced from the current experimental work.

3.6. Cell growth and viability in the presence of nanofibers

We firstly investigated the effect of the different sheets materials on the viability of the HEK cells. A given number of cells (5×10^4 mL^{-1}) were cultivated in 24-well plates in the absence (control), and in the presence of different sheet discs (5 mm in diameter), for 4 days. The metabolic activities of the cells were then measured using MTT-assay, as described in the method section. In general, PLA sheets were floating on the surface of cultivation media during the first 24 h of cultivation then they went to the bottom of the cultivation wells. It could be because of the known hydrophobic nature of this polymer. In comparison, PVA sheets, as well as, sheets that have PVA as a peripheral shell, were unstable in the cultivation media, they started to shrink during the first 24 h of cultivation. Regarding the metabolic activities of the cells in the presence of different sheets material, as shown in Fig. 9, PVA sheets exhibited the most unsuitable sheets HEK cells proliferation; the metabolic activity of the cells did not exceed 20% in comparison to the control cells. The reason could be the apparent instability of PVA in aqueous solution. In contrast, the metabolic activity of HEK cells in the presence of PLA nanofiber sheets was only affected by 25%, (Fig. 9). However, cells growing in the presence of a mixture that contains PVA as core and PLA as a shell or vice versa showed considerable better material for cell growth behavior than PVA alone. The metabolic activities of HEK cells were about 40%.

We further investigated the attachment of HEK cells to the different nanofiber materials using SEM technique. HEK cells were allowed to grow on the nanofiber surfaces for 4 days, after that the nanofibers samples were prepared for SEM investigation as described in the method section. In general, we could observe relatively good attachment of the cells on pure PLA nanofiber (Fig. 10C1–C3), as well as, on the core/shell-structured nanofibers of PLA/PVA (Fig. 10A1–A3), and PVA/PLA (Fig. 10B1–B3). In contrast, the attachment of cells to the PVA nanofibers mat was the worst between the groups (Fig. 10D1–D3). The reason for bad attachment could be attributed to the poor stability of PVA polymer in aqueous environment as mentioned above. In conclusion, using a mixture of PLA and PVA seems to increase the ability of PVA for cell attachment, and consequentially, increases its chance for biomedical applications.

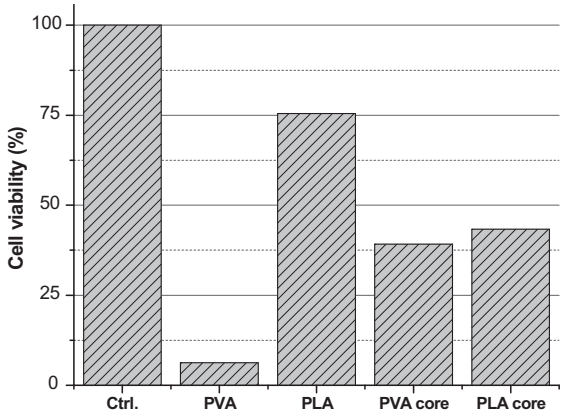

Fig. 9. The cell viability in the presence of different nanofiber mat materials.

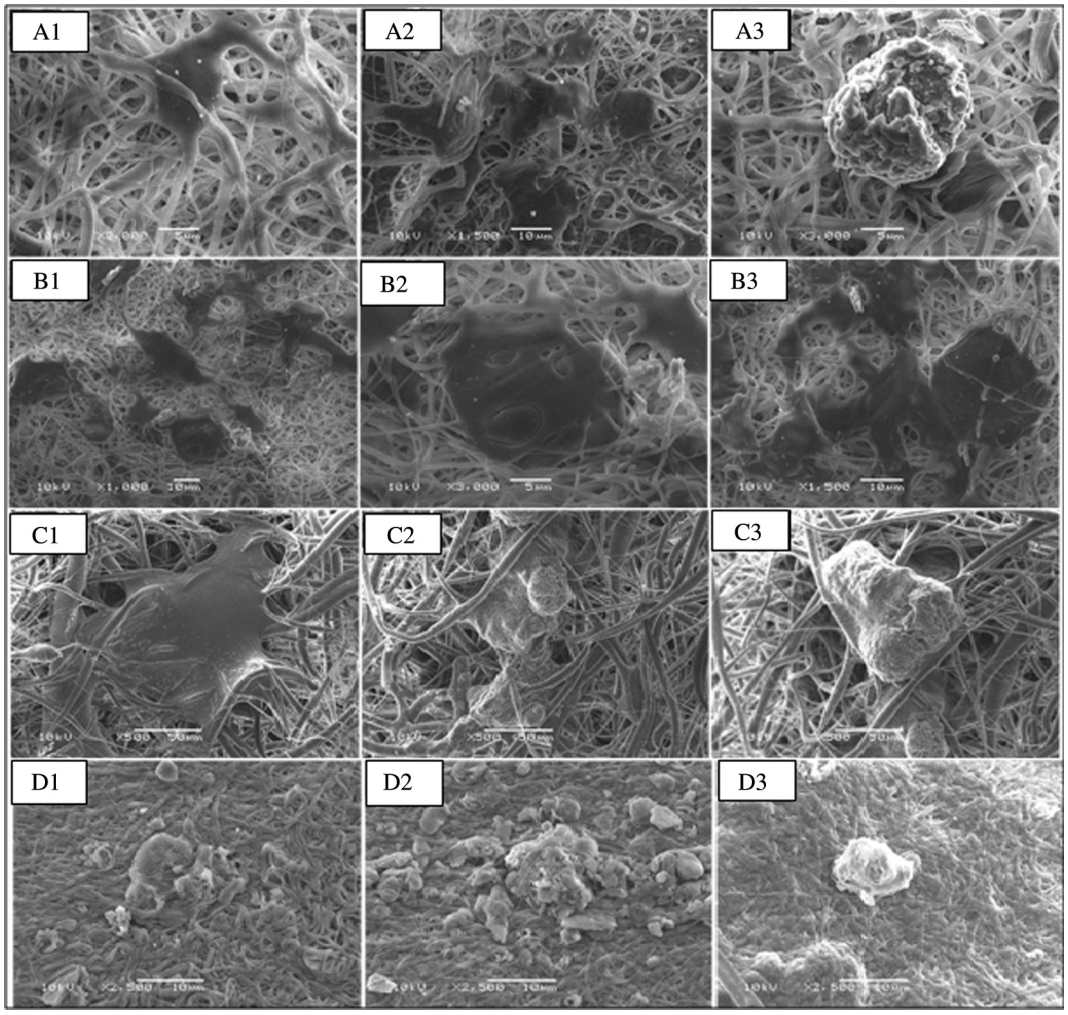

Fig. 10. SEM of HEK cells attachment. A1-A3 = core/shell-structured PLA/PVA, B1-B3 = core/shell-structured PVA/PLA, C1-C3 = pristine PLA, and D1-D3 = pristine PVA. Each row in the figure shows different locations and/or magnification for the same material.

4. Conclusions

In this study, we successfully fabricated core-shell composite nanofibers composed of PLA and PVA by coaxial electrospinning technique. The significant improvements in the surface wetting and mechanical properties were achieved for the composite structure when using PLA in the core and PVA in the shell. The core/shell nature of the synthetic nanofiber sheets were confirmed by SEM and TEM techniques with average diameters of about 35 ± 5 nm and 165 ± 10 nm for the core and shell, respectively. Further, the DSC, TGA, and FTIR analyses of the composite nanofibers shows characteristics of both PLA and PVA, which provide further evidence for the successful fabrication of core/shell composite nanofibers via coaxial electrospinning. The core/shell-structured PLA/PVA nanofiber mats displayed enhanced hydrophilicity with a water contact angle of 27 ± 1.5° compared to 110° ± 2.5° for pristine PLA. The composite nanofibers possess a tensile strength of 14.5 MPa and a strain at failure of about 110%, which represent nearly 254% and 175% increase compared to those of pristine PLA. Moreover, the metabolic activities of human embryonic kidney cells (HEK-293) and the attachment of the cells to the different nanofiber materials produced in this study were investigated. It is found that the core-shell PLA/PVA composite nanofiber scaffolds exhibited good cell growth behavior and increased ability for cell attachment. Therefore, the new coaxial PLA/PVA composite scaffold has the potential to be a candidate material in biomedical applications owing to its excellent mechanical, surface wetting, and cytocompatibility properties.

Acknowledgements

The authors extend their appreciation to the Deanship of Scientific Research at King Saud University for funding this work through Research Group no. RGP-1438-035.

Appendix A. Supplementary material

Supplementary data associated with this article can be found, in the online version, at http://dx.doi.org/10.1016/j.eurpolymj.2017.11.052.

References

[1] T.H. Qazi, R. Rai, A.R. Boccaccini, Tissue engineering of electrically responsive tissues using polyaniline based polymers: a review, Biomaterials 35 (33) (Nov. 2014) 9068–9086.
[2] A. Rogina, Electrospinning process: versatile preparation method for biodegradable and natural polymers and biocomposite systems applied in tissue engineering and drug delivery, Appl. Surf. Sci. 296 (Mar. 2014) 221–230.
[3] A. Abdal-hay, F.A. Sheikh, J.K. Lim, Air jet spinning of hydroxyapatite/poly(lactic acid) hybrid nanocomposite membrane mats for bone tissue engineering, Colloids Surf. B Biointerfaces 102 (Feb. 2013) 635–643.
[4] M. Angeles, H.-L. Cheng, S.S. Velankar, Emulsion electrospinning: composite fibers from drop breakup during electrospinning, Polym. Adv. Technol. 19 (7) (2008) 728–733.
[5] R.M. Rasal, A.V. Janorkar, D.E. Hirt, Poly(lactic acid) modifications, Prog. Polym. Sci. 35 (3) (2010) 338–356.
[6] S.A. Arvidson, K.C. Wong, R.E. Gorga, S.A. Khan, Structure, molecular orientation, and resultant mechanical properties in core/sheath poly(lactic acid)/polypropylene composites, Polymer 53 (3) (2012) 791–800.

[7] C.P. Barnes, S.A. Sell, E.D. Boland, D.G. Simpson, G.L. Bowlin, Nanofiber technology: designing the next generation of tissue engineering scaffolds, Adv. Drug Deliv. Rev. 59 (14) (2007) 1413–1433.
[8] Y. Su, et al., Controlled release of bone morphogenetic protein 2 and dexamethasone loaded in core-shell PLLACL-collagen fibers for use in bone tissue engineering, Acta Biomater. 8 (2) (2012) 763–771.
[9] H. Zhang, H. Nie, S. Li, C.J.B. White, L. Zhu, Crosslinking of electrospun polyacrylonitrile/hydroxyethyl cellulose composite nanofibers, Mater. Lett. 63 (13) (2009) 1199–1202.
[10] S. Sarapirom, L.D. Yu, D. Boonyawan, C. Chaiwong, Effect of surface modification of poly(lactic acid) by low-pressure ammonia plasma on adsorption of human serum albumin, Appl. Surf. Sci. 310 (2014) 42–50.
[11] J.M. Goddard, J.H. Hotchkiss, Polymer surface modification for the attachment of bioactive compounds, Prog. Polym. Sci. 32 (7) (2007) 698–725.
[12] E. Stoleru, et al., Novel procedure to enhance PLA surface properties by chitosan irreversible immobilization, Appl. Surf. Sci. 367 (2016) 407–417.
[13] K. Rezwan, Q.Z. Chen, J.J. Blaker, A.R. Boccaccini, Biodegradable and bioactive porous polymer/inorganic composite scaffolds for bone tissue engineering, Biomaterials 27 (18) (2006) 3413–3431.
[14] Z. Yang, J. Si, Z. Cui, J. Ye, X. Wang, Q. Wang, et al., Biomimetic composite scaffoldsbased on surface modification of polydopamine on electrospun poly(lactic-cacid)/cellulose nanofibrils, Carbohydr. Polym. 174 (Supplement C) (2017) 750–759.
[15] A. Abdal-hay, K.H. Hussein, L. Casettari, K.A. Khalil, A.S. Hamdy, Fabrication of novel high performance ductile poly(lactic acid) nanofiber scaffold coated with poly (vinyl alcohol) for tissue engineering applications, Mater. Sci. Eng. C 60 (Mar. 2016) 143–150.
[16] Y. Wang, J. Qian, T. Liu, W. Xu, N. Zhao, A. Suo, Electrospun PBLG/PLA nanofiber membrane for constructing in vitro 3D model of melanoma, Mater. Sci. Eng. C 76 (Jul. 2017) 313–318.
[17] M. Hiljanen-Vainio, P. Varpomaa, J. Seppälä, P. Törmälä, Modification of poly(L-lactides) by blending: mechanical and hydrolytic behavior, Macromol. Chem. Phys. 197 (4) (1996) 1503–1523.
[18] R.M. Rasal, D.E. Hirt, Toughness decrease of PLA-PHBHHx blend films upon surface-confined photopolymerization, J. Biomed. Mater. Res. A 88 (4) (2009) 1079–1086.
[19] H. Tsuji, Poly(Lactic Acid), in: S. Kabasci (Ed.), Bio-Based Plastics, John Wiley & Sons Ltd., 2013, pp. 171–239.
[20] Z.-M. Huang, Y.-Z. Zhang, M. Kotaki, S. Ramakrishna, A review on polymer nanofibers by electrospinning and their applications in nanocomposites, Compos. Sci. Technol. 63 (15) (2003) 2223–2253.
[21] S. Farah, D.G. Anderson, R. Langer, Physical and mechanical properties of PLA, and their functions in widespread applications—a comprehensive review, Adv. Drug Deliv. Rev. 107 (2016) 367–392.
[22] S.C. Cifuentes, E. Frutos, R. Benavente, V. Lorenzo, J.L. González-Carrasco, Assessment of mechanical behavior of PLA composites reinforced with Mg microparticles through depth-sensing indentations analysis, J. Mech. Behav. Biomed. Mater. 65 (2017) 781–790.
[23] C.-Y. Wang, J.-J. Liu, C.-Y. Fan, X.-M. Mo, H.-J. Ruan, F.-F. Li, The effect of aligned core-shell nanofibres delivering NGF on the promotion of sciatic nerve regeneration, J. Biomater. Sci. Polym. Ed. 23 (1–4) (2012) 167–184.
[24] S. Agarwal, J.H. Wendorff, A. Greiner, Use of electrospinning technique for biomedical applications, Polymer 49 (26) (2008) 5603–5621.
[25] D.-G. Yu, J.-H. Yu, L. Chen, G.R. Williams, X. Wang, Modified coaxial electrospinning for the preparation of high-quality ketoprofen-loaded cellulose acetate nanofibers, Carbohydr. Polym. 90 (2) (2012) 1016–1023.
[26] S.I. Jeong, et al., In vivo biocompatibilty and degradation behavior of elastic poly(L-lactide-co-epsilon-caprolactone) scaffolds, Biomaterials 25 (28) (2004) 5939–5946.
[27] A.K. Moghe, B.S. Gupta, Co-axial electrospinning for nanofiber structures: preparation and applications, Polym. Rev. 48 (2) (2008) 353–377.
[28] Z. Sun, E. Zussman, A.l. Yarin, J.h. Wendorff, A. Greiner, Compound core-shell polymer nanofibers by co-electrospinning, Adv. Mater. 15 (22) (2003) 1929–1932.
[29] N.H.A. Ngadiman, N.M. Yusof, A. Idris, D. Kurniawan, Mechanical properties and biocompatibility of co-axially electrospun polyvinyl alcohol/maghemite, Proc. Inst. Mech. Eng. [H] 230 (8) (2016) 739–749.
[30] T. Mosmann, Rapid colorimetric assay for cellular growth and survival: application to proliferation and cytotoxicity assays, J. Immunol. Methods 65 (1–2) (1983) 55–63.
[31] E.A. Schmitt, D.R. Flanagan, R.J. Linhardt, Importance of distinct water environments in the hydrolysis of poly(DL-lactide-co-glycolide), Macromolecules 27 (3) (Jan. 1994) 743–748.
[32] A.G. Mikos, N.A. Peppas, Polymer chain entanglements and brittle fracture: 2. Autohesion of linear polymers, Polymer 30 (1) (1989) 84–91.
[33] V.M. Merkle, L. Zeng, M.J. Slepian, X. Wu, Core-shell nanofibers: integrating the bioactivity of gelatin and the mechanical property of polyvinyl alcohol, Biopolymers 101 (4) (2014) 336–346.
[34] X.-H. Qin, S.-Y. Wang, Electrospun nanofibers from crosslinked poly(vinyl alcohol) and its filtration efficiency, J. Appl. Polym. Sci. 109 (2) (2008) 951–956.
[35] Z.-R. You, M.-H. Hu, H.-Y. Tuan-Mu, J.-J. Hu, Fabrication of poly(glycerol sebacate) fibrous membranes by coaxial electrospinning: Influence of shell and core solutions, J. Mech. Behav. Biomed. Mater. 63 (2016) 220–231.
[36] G. Kister, G. Cassanas, M. Vert, B. Pauvert, A. Térol, Vibrational analysis of poly(L-lactic acid), J. Raman Spectrosc. 26 (4) (1995) 307–311.
[37] R.P. Gonçalves, F.F.F. da Silva, P.H.S. Picciani, M.L. Dias, Morphology and thermal properties of core-shell PVA/PLA ultrafine fibers produced by coaxial electrospinning, Mater. Sci. Appl. 06 (02) (2015) 189.
[38] Z.-M. Huang, Y. Zhang, S. Ramakrishna, Double-layered composite nanofibers and their mechanical performance, J. Polym. Sci. Part B Polym. Phys. 43 (20) (2005) 2852–2861.
[39] V. Merkle, L. Zeng, W. Teng, M. Slepian, X. Wu, Gelatin shells strengthen polyvinyl alcohol core–shell nanofibers, Polymer 54 (21) (2013) 6003–6007.
[40] M.P. Prabhakaran, J. Venugopal, S. Ramakrishna, Electrospun nanostructured scaffolds for bone tissue engineering, Acta Biomater. 5 (8) (2009) 2884–2893.
[41] B. Sun, B. Duan, X. Yuan, Preparation of core/shell PVP/PLA ultrafine fibers by coaxial electrospinning, J. Appl. Polym. Sci. 102 (1) (2006) 39–45.